Variation in the Composition and In Vitro Proinflammatory Effect of Urban Particulate Matter from Different Sites

Natalia Manzano-León,[1] *Raúl Quintana,*[1] *Brisa Sánchez,*[2] *Jesús Serrano,*[3] *Elizabeth Vega,*[4] *Inés Vázquez-López,*[1] *Leonora Rojas-Bracho,*[5] *Tania López-Villegas,*[5] *Marie S. O'Neill,*[2] *Felipe Vadillo-Ortega,*[6] *Andrea De Vizcaya-Ruiz,*[7] *Irma Rosas,*[8] *and Álvaro R. Osornio-Vargas*[1,9]

[1]Instituto Nacional de Cancerología, Av. San Fernando 22, Col. Sección XVI, C.P. 14080, México, D.F., México

[2]Departments of Environmental Health Sciences and Epidemiology, University of Michigan, School of Public Health, Ann Arbor, MI 48109, USA

[3]Facultad de Ciencias, Universidad Nacional Autónoma de México, C.P. 04510, México, D.F. México

[4]Instituto Mexicano del Petroleo, Eje Central Lázaro Cárdenas 152, Edif. 27D, Cubículo 110, San Bartolo Atepehuacan, C.P. 07730, México, D.F. México

[5]Instituto Nacional de Ecología, Periférico Sur 5000, 4to piso, Col. Insurgentes Cuicuilco, C.P. 04530, México, D.F. México

[6]Universidad Nacional Autónoma de México, Branch at National Institute of Genomic Medicine, Periferico Sur 4809, Col. Arenal Tepepan, C.P. 14610, México, D.F. México

[7]Departamento de Toxicología, Cinvestav, Av. Instituto Politécnico Nacional 2508, San Pedro Zacatenco, C.P. 07360, México, D.F. México

[8]Centro de Ciencias de la Atmósfera, Universidad Nacional Autónoma de México, Circuito Exterior s/n. Ciudad Universitaria, Del. Coyoacán, C.P. 04510, México, D.F. México

[9]Department of Paediatrics, University of Alberta, Edmonton, Canada, 3-591 ECHA, NW. Edmonton T6G 1C9, Canada; E-mail: *osornio@ualberta.ca*

Received 31 October 2012; revised 6 December 2012; accepted 8 December 2012

ABSTRACT: Spatial variation in particulate matter–related health and toxicological outcomes is partly due to its composition. We studied spatial variability in particle composition and induced cellular responses in Mexico City to complement an ongoing epidemiologic study. We measured elements, endotoxins, and polycyclic aromatic hydrocarbons in two particle size fractions collected in five sites. We compared the in vitro proinflammatory response of J774A.1 and THP-1 cells after exposure to particles, measuring subsequent TNFα and IL-6 secretion. Particle composition varied by site and size. Particle constituents were subjected to principal component analysis, identifying three components: C_1 (Si, Sr, Mg, Ca, Al, Fe, Mn, endotoxin), C_2 (polycyclic aromatic hydrocarbons), and C_3 (Zn, S, Sb, Ni, Cu, Pb). Induced TNFα levels were higher and more heterogeneous than IL-6 levels. Cytokines produced by both cell lines only correlated with C_1, suggesting that constituents associated with soil induced the inflammatory response and explain observed spatial differences. © 2013 Wiley Periodicals, Inc. J Biochem Mol Toxicol 27:87–97, 2013; View this article online at wileyonlinelibrary.com. DOI 10.1002/jbt.21471

KEYWORDS: **Particulate Matter (PM); Chemical Composition; Spatial Variation; Cytokines; Soil**

INTRODUCTION

Health effects associated with air pollution have been studied in various cities around the world [1]. The epidemiological evidence has pointed to particulate matter (PM) as the pollutant that best represents the mixture of pollutants in air and is most consistently correlated with adverse health effects [2]. Recent studies have found significant heterogeneity of PM-associated

Correspondence to: Álvaro R. Osornio-Vargas.

The authors declare that there are no conflicts of interest.

Contract Grant Sponsor: Fogarty International Research Collaboration Award (FIRCA).

Contract Grant Sponsor: National Institute for Environmental Health Sciences (NIEHS)

Contract Grant Numbers: R01 ES016932 and R01 ES017022-01.

Contract Grant Sponsor: Instituto Nacional de Ecología (INE-Mexico).

health effects across cities or regions [3–6]. These differences seem to be related not only to PM size or mass but also to the distinct chemical composition of the particle mixture in different locations [4, 5]. More recent epidemiological studies have analyzed health outcomes associated with estimated exposure to PM-related constituents (e.g., organic and elemental carbon, ions, and metals), in addition to the standard PM mass metrics (particles below 10 or 2.5 μm in aerodynamic diameter, PM_{10} and $PM_{2.5,}$ respectively) [7, 8]. For example, cardiovascular effects have been associated with the particle number concentration whereas respiratory outcomes were linked with $PM_{2.5}$ content of sodium and ammonium nitrate, sulfate, chloride, and organic carbon [9], and diabetes complications with arsenic, organic carbon, and sulfate in $PM_{2.5}$ [10]. These findings support the idea that particle composition is a key determinant of the observed location-specific variability in epidemiologic associations.

Experimental studies have examined effects on animals and cells in relation to PM chemical composition. A controlled exposure study performed in mice [11] showed an increase in lung inflammatory cells associated with iron content in coarse PM. In vitro cell studies found a relation between the secretion of inflammatory proteins and the coarse, fine, and quasi-ultrafine PM content of endotoxin, iron, and copper [12, 13]. Consistent with findings from epidemiological studies, toxicological studies also show that, in addition to PM size, site differences in PM composition within a city influence cytokine secretion patterns [14, 15].

Currently, few studies simultaneously explore toxicological and epidemiological evidence to address the role of spatial variation in PM composition and human health outcomes. We are particularly interested in mechanisms underlying observed associations between air pollution and birth outcomes in epidemiologic studies. Several biological mechanisms have been hypothesized to mediate this association, including inflammation, oxidative stress, coagulation, endothelial function, and hemodynamic responses, and different mechanisms are probably involved at various stages of pregnancy [16]. In this paper, we discuss toxicological experiments designed to shed light on PM-related proinflammatory potential involved that could play a role in observed associations between air pollution and birth outcomes at the population level.

This study assessed spatial variability in PM_{10} and $PM_{2.5}$ chemical composition and toxic effects, using multiple PM samples collected during 4 months at five different sites of Mexico City. Specifically, we were interested in developing evidence on how air pollution may contribute to inflammation during pregnancy, leading to perinatal complications such as preterm birth, using both toxicological approaches and epidemiological evidence in a study we are conducting in Mexico City and described elsewhere [17]. In the present study, we explore the use of frequent, repeated samples to enhance our ability to study spatial variability in PM composition. We measured toxicological responses in two cell lines, a human (THP-1 cells) and a murine (J774A.1 cells) one, to assess their comparability, since reports using both cell lines exist in the literature [14, 15, 18, 19]. We evaluated the elements present in PM, as well as content of polycyclic aromatic hydrocarbons (PAH) and endotoxin.

MATERIALS AND METHODS

PM_{10} and $PM_{2.5}$ Sampling

PM_{10} and $PM_{2.5}$ were collected simultaneously at five sites in Mexico City using high volume samplers (GMW model 1200 VFC HVPM10; Sierra Andersen, Smyrna, GA or Tisch TE6070V, Roswell, GA), and nitrocellulose membranes. Integrated 24 h samples were collected from May 18 through August 7 of 2009, every Monday, Wednesday, and Friday. The air was pumped at a rate of 1.13 m^3/min across nitrocellulose membranes with a nominal pore size of 3 μm (11302-131; Sartorius, Goettingen, Germany). The membranes were prepared as described previously [20].

The particles were mechanically recovered from the membranes using a surgical blade. To have enough PM for analysis and experimentation, samples from three consecutive weeks were pooled by site and size. Pooled PM samples were stored in glass vials in the dark at 4°C, according to previously published methods [20]. Over the course of 12 weeks, this yielded four samples per site and size fraction, resulting in 40 samples. Each one of them was used to determine composition and proinflammatory potential.

The five sampling sites were selected according to the main activities occurring in their surroundings, accessibility, and proximity to official monitoring stations of the Mexico City government network [21]. This sitting allowed us to access data on atmospheric levels of criteria pollutants and meteorological data in the immediate vicinity of our samplers. We collected PM_{10} and $PM_{2.5}$ in the industrial sector of the city, located in the north (Industrial-North, I-N), a business area located in the center of the city (Business-Center, B-C), and three residential zones in the south (Residential-South, R-S), east (Residential-East, R-E), and west (Residential-West, R-W) of Mexico City. Traffic is the main source of pollution in these residential areas. The region in the east is the most populated and has the poorest urban infrastructure, whereas the one in the west represent the least polluted of the three [22].

Determination of Elements by Mass Spectrometry with Inductively Coupled Plasma

One milligram of PM was resuspended in 3 mL of American Society for Testing and Materials type 1 deionized water (18.2 MΩ/cm Quantum^{TM} ICP cartridge and filter of 0.1 μm, Millipore R), and the suspension was passed through a GNWP nylon filter (0.2 μm; Millipore). Filtered samples were analyzed for Li, Na, Mg, Al, Si, S, K, Ca, Sc, V, Cr, Mn, Fe, Co, Ni, Cu, Zn, As, Rb, Sr, Y, Mo, Ag, Sb, Ba, Ce, and Pb using inductively coupled plasma mass spectrometry (ICP-MS) (Agilent 7500a). Analysis conditions were 3 scans, 32 channels, 100 passes, incident power of 1.39 kW, RF matching 1.76 V, nebulizer gas (1.0 L/min flow), spray chamber (temperature of 2°C), and a discriminator (9.5 mV).

Filtered samples in solution were introduced by pneumatic nebulization into radiofrequency plasma where energy transfer processes cause desolvation, atomization, and ionization. The ions are extracted from the plasma through a differentially pumped vacuum interface and separated on the basis of their mass-to-charge (m/z) ratio by a mass spectrometer. An electron multiplier or Faraday detector detects ions transmitted through the mass analyzer, and a data handling system processes the resulting current. Interference equations were used for corrections in all samples. The method for validating the parameters includes linearity ($R^2 <$ 0.99), reproducibility, and repeatability (coefficient of variation <2%). The limit of detection was between 1.6 ppb (Li) to 15.7 ppb (Hg). The limit of quantification varies for each compound [23].

Determination of Polycyclic Aromatic Hydrocarbons by High Performance Liquid Chromatography

One milligram of each PM sample was extracted with 30 mL of dichloromethane in a microwave oven (CEM, model MarsX) with a power of 1200 W, pressure of 100 psi, and a temperature of 115°C. Subsequently, the extracts were concentrated to 1 mL with an ultra pure nitrogen stream using a nitro evaporator (8158, NEVAP 111; Organomation Associates, Inc). The solvent was changed to acetonitrile, and the extracts were filtered to 0.2 μm acrodisc (Pall Gelman Laboratory) and concentrated to 0.5 mL samples under an ultra pure nitrogen stream. The extracts were analyzed for naphtalene, acenaphthylene, acenaphthene, fluorene, phenanthrene, anthracene, fluoranthene, pyrene, benzo(a)anthracene, chrysene, benzo(b)fluoranthene, benzo(k)fluoranthene, benzo(a)pyrene, dibenzo(a,h)anthracene, benzo(g,h,i) perylene, and indene with a liquid chromatograph (Agilent HP, 1100 series) equipped with a Nucleosil column (Macherey-Nagel, 265 mm; 100-5 C18 PAH), with automatic sample injector and a fluorescent detector. 4,4′-Difluorobiphenyl was added to all samples as an internal standard, and results were calculated after subtracting baseline readings [24].

Determination of Endotoxins by Using the Limulus Amebocyte Lysate Colorimetric Method

PM was resuspended in 50 mM Tris buffer (1 mg/mL), sonicated for 1 h at 22°C, with intervals of agitation in vortex for 1 min every 15 min. We used three 1:5 serial dilutions with the same buffer, using glassware baked at 250°C/4 h and disposable micropipette tips free of endotoxins. The quantitative method of limulus amebocyte lysate Kinetic-QCL was performed as specified by the supplier. The samples were analyzed in duplicate in sterile 96-well microplates, free of endotoxins. The endotoxin concentration was determined using the Kinetic-QCL reader connected to a computer containing a software Kinetic-QCL and a reference curve with a standard endotoxin from *Escherichia coli* O55:B5 with an output of 7 endotoxin units (EU) per nanogram (ng). This equipment keeps the samples at 37°C, and the absorbance of the microplate at 405 nm was monitored every 150 s.

Cell Culture

We used J774A.1 cells (monocytes/macrophages from mice) and THP-1 cells (human monocytic cell line), obtained from the American Type Culture Collection (ATCC). Cells were cultured in 10% fetal bovine serum–DMEM (Dulbecco's modified Eagle's media) or RPMI (Cat. A10491; Sigma), respectively. Both media contained penicillin (50 U/mL)/streptomycin (50 μg/mL). Cultures were kept at 37°C in a 5% CO_2/95% air atmosphere.

Proinflammatory Cytokines, Acute (TNFα), and Chronic (IL-6) Phase

Tumor necrosis factor α (TNFα) and interleukin-6 (IL-6) were measured in the supernatants of confluent cultures of J774A.1 and THP-1 cells (550,000/mL) maintained in serum-free medium for 24 h. They were then exposed to 80 μg/mL of the PM_{10} or $PM_{2.5}$ samples obtained from different sites for an additional 24 h. One mg/mL PM aliquots were prepared just before exposing the cells, vortexed, sonicated in a water bath

sonicator for 5 min, and resuspended three times before adding the final concentration to the cell culture to attain a homogeneous suspension. Subsequently, the enzyme-linked immunosorbent assay (ELISA) method measured the presence of cytokines in the supernatants. Each one of the 3-week pooled samples was tested in three independent experiments. ELISA results from each experiment are the average of the results obtained from two wells. We used commercial kits, R&D Systems (Minneapolis, MN) for mouse samples and Invitrogen (Carlsbad, CA) for human cytokines. Nonexposed cells were used as negative controls, and cells exposed to lipopolysaccharide (LPS) (10 μg/mL) were used as positive controls. The results are expressed in pg/mL. The concentration of 80 μg/mL was chosen based on previous work from our lab where we found an increased inflammatory response without loss of cell viability at this level of exposure [14, 15].

Statistical Analysis

As described above, PM_{10} and $PM_{2.5}$ samples were collected over the course of 12 weeks at each of the selected five sites. Samples from 3 weeks were pooled to have enough PM for chemical analyses and experimentation, resulting in four samples per site and PM size ($n = 40$). PM composition was determined by site and PM size, and summary statistics were computed for each PM constituent (27 elements, 16 PAHs, and endotoxin). Owing to the skewed distribution of the constituents, Kruskal–Wallis one-way analysis of variance (ANOVA) was used to test for differences in their distribution across sites within each PM size, and the Mann–Whitney rank sum test was used to compare across PM fractions.

Principal component analysis (PCA) was used to reduce dimensionality of PM constituents. We included data from both PM sizes considering that (1) we only had a sample equal to 20 for each PM size and (2) composition (not constituents' concentrations) is basically the same for both PM fractions. Prior to PCA, all constituents were natural log transformed given their highly skewed distributions. Principal components with eigenvalue >1 were extracted, and component scores were computed by summing standardized concentrations for constituents with factor loadings greater than 0.6 [25]. Statistical differences of component scores across sites within PM size were tested by the Kruskal–Wallis one-way ANOVA test. Pairwise differences between any two sites were tested with the Mann–Whitney rank sum test.

Measurements of the in vitro proinflammatory toxicological responses (IL-6 and TNFα for each cell line) were compared across sites using Kruskal–Wallis nonparametric ANOVA and across PM size using Mann–Whitney rank sum tests. Pairwise differences between any two sites were tested with the Mann–Whitney rank sum test. Partial Spearman correlations (adjusted for PM size) between principal component scores and toxicological responses were used to assess their relationships with toxicological responses and to assess the similarity in toxicological responses across cell types exposed to PM collected at the same location and time.

RESULTS

Chemical Composition of PM_{10} and $PM_{2.5}$

Twenty-seven elements were determined in the PM samples collected in the five sampling sites. Table 1 presents the average values and standard deviations of elements in each area; constituents for which at least one zone was found to be different from the others ($p < 0.05$, KW ANOVA) are denoted with an asterisk (*). The percentage of PM mass explained by all these elements varied by site; between 9% and 18% for PM_{10} and 1.8–6% for $PM_{2.5}$. Both PM fractions had a high content of Ca, S, Na, K, Si, Mg, Cu, Al, and Fe. PM_{10} from R-S had higher concentrations of S, K, Cu, and Zn, whereas $PM_{2.5}$ from the same region had higher levels of Ca, Si, and Al. The analysis of PAH (Table 2) demonstrated that acenaphthylene and phenanthrene were the most commonly represented PAHs in both PM fractions, and higher concentrations were found for PM_{10} ($p < 0.05$). Other PAHs were present in PM samples in very small concentrations. Total average PAH concentrations were 49.77 ng/mg for PM_{10} and 34.37 ng/mg for $PM_{2.5}$ ($p > 0.05$).

Endotoxin was present in all samples studied. Concentrations were significantly higher in PM_{10} than in $PM_{2.5}$ ($p < 0.05$). PM_{10} did not show significant differences by site ($p > 0.05$), but $PM_{2.5}$ did ($p < 0.05$) (Table 3). Interestingly, both PM fractions from R-S had similar levels of endotoxin ($p > 0.05$)

Principal Components Analysis

The first three principal components extracted by the PCA explained 69.9% of the total variance. The components included the following constituents: first component (C_1): Si, Sr, Mg, Ca, Al, Fe, Mn, Ba, and endotoxin; second component (C_2): pyrene, fluoranthene, chrysene, benzo(a)anthracene, benzo(b)fluoranthene, and benzo(k)fluoranthene, Li, Cr, and As; and the third component (C_3): Zn, S, Sb, Ni, Cu, Pb, and K (Table 4).

TABLE 1. Descriptive Statistics for Elements in PM_{10} and $PM_{2.5}$ Samples

	PM_{10} (ng/mg)											$PM_{2.5}$ (ng/mg)									
	R-W		I-N		B-C		R-S		R-E			R-W		I-N		B-C		R-S		R-E	
Elements	Average	SD	Average	SD	Average	SD	Average	SD	Average	SD	Elements	Average	SD	Average	SD	Average	SD	Average	SD	Average	SD
Ca	86,894.7	3,647.1	89,408.9	7,445.5	94,716.6	15,132.0	126,691.5	48,955.0	69,697.6	31,470.8	Ca*	11,280.9	6,866.9	6,574.4	4,878.2	8,764.6	7,763.6	46,655.5	16,940.3	4,875.8	3,130.4
S*	9,050.0	1,913.0	17,682.6	372.6	12,111.1	2,329.5	30,933.3	14,853.6	12,469.5	3,409.1	S	4,227.7	2,411.7	4,189.0	1,931.7	5,951.1	1,585.1	7,109.2	4,573.6	4,926.8	1,800.3
Na	6,066.9	1,800.6	7,760.5	1,964.8	6,903.6	1,713.0	8,785.1	5,217.3	4,750.4	475.1	Na	3,482.6	1,026.4	4,667.2	1,162.8	4,924.9	1,050.6	4,188.6	1,556.2	4,104.5	951.8
K*	1,759.0	306.5	3,000.9	815.1	2,011.2	484.0	4,076.7	1,315.9	2,047.9	1,032.8	K	739.5	545.4	847.7	755.1	850.8	347.6	971.4	528.3	791.4	526.4
Si	2,160.6	301.8	1,742.7	144.2	2,496.7	1,654.8	1,672.0	501.6	1,579.5	548.9	Si*	228.3	212.0	142.7	110.7	192.1	77.2	1,142.4	579.1	0.0	0.0
Mg	1,138.6	55.1	1,366.1	191.1	1,424.9	323.2	1,743.8	788.6	1,186.8	377.3	Mg	217.7	125.6	159.0	45.5	287.0	113.7	750.4	276.7	180.4	70.7
Cu*	144.6	28.4	228.5	102.7	172.7	61.2	3,665.0	2,187.8	197.6	122.2	Zn	177.7	103.0	362.7	147.2	239.7	42.1	153.9	96.5	198.6	55.7
Al	839.9	112.6	590.0	23.3	1,030.8	896.9	806.0	213.5	663.9	185.9	Cu	251.4	205.6	129.5	55.2	82.1	31.7	228.3	158.7	296.7	162.2
Fe	598.7	67.2	588.1	79.5	820.2	555.7	842.4	294.7	527.7	144.6	Al*	110.7	68.4	53.6	25.3	99.5	24.4	565.2	293.8	86.7	20.1
Zn*	78.6	44.0	763.6	341.7	336.4	215.3	1,342.7	917.2	169.6	127.2	Fe	97.3	96.2	142.0	106.3	113.9	35.2	410.7	212.7	94.7	30.7
V*	104.9	60.9	197.2	77.2	128.0	44.7	208.8	100.9	95.4	49.6	V	39.7	21.4	45.2	30.1	42.7	15.3	61.5	40.1	30.4	21.2
Ba	109.9	8.6	116.7	29.4	126.5	29.3	279.7	178.8	78.0	9.7	Mn*	23.2	17.4	39.5	35.7	20.3	5.9	69.2	29.0	17.5	4.5
Sr	110.4	11.1	124.5	15.3	145.0	27.2	183.4	83.0	113.6	52.6	Ba	31.5	25.6	15.9	12.7	23.2	11.6	67.7	23.9	19.8	7.1
Mn*	75.7	20.0	159.3	30.1	111.5	23.2	215.4	113.2	85.1	5.2	Sr*	16.5	13.0	6.8	4.7	13.8	9.7	63.5	20.7	8.6	3.4
Sb*	14.0	2.5	32.7	5.5	28.1	9.3	46.1	30.8	24.7	4.3	Pb*	18.6	13.3	34.5	17.4	19.0	8.1	7.1	3.1	11.8	3.2
Ni*	12.6	10.5	20.6	10.2	12.3	3.4	31.5	15.0	9.4	2.2	Sb	13.4	8.6	17.6	9.8	18.1	7.8	9.8	5.0	16.9	5.0
Pb*	7.2	1.5	24.4	8.4	17.7	7.7	26.2	13.1	8.7	1.9	As	10.4	11.0	13.7	12.5	9.1	8.2	5.0	3.8	3.7	2.9
As	10.5	7.9	26.3	17.0	16.7	8.5	17.3	9.5	8.8	5.1	Ni	10.0	6.9	7.1	4.3	6.8	2.4	9.7	8.2	6.0	5.1
Cr	6.1	1.1	19.5	6.8	7.3	1.6	12.5	7.3	6.9	3.1	Cr*	6.1	4.4	12.3	5.2	3.3	1.3	4.8	1.8	1.5	0.4
Mo*	4.9	1.1	11.1	1.5	6.7	2.0	10.4	6.3	3.9	0.9	Li*	5.3	4.0	9.5	3.4	1.5	0.5	0.7	0.6	0.1	0.2
Li*	1.3	0.6	14.6	6.5	3.2	1.2	2.4	1.7	0.8	0.5	Mo	5.0	4.0	3.2	2.0	1.7	0.5	2.8	1.3	1.1	0.2
Rb*	2.9	0.3	4.5	0.7	3.2	1.2	5.6	1.8	2.6	1.3	Rb	4.3	3.9	0.7	0.8	0.6	0.5	1.4	1.0	0.4	0.5
Co	0.7	0.7	1.0	0.1	1.0	0.3	2.5	1.3	0.5	0.1	Co	N/D		N/D		N/D		0.7	0.4	N/D	
Ce	0.4	0.3	0.5	0.2	0.7	0.7	0.8	0.6	0.3	0.3	Ag	N/D		N/D		N/D		0.7	0.0	N/D	
Y	0.1	0.1	0.2	0.2	0.3	0.0	0.7	0.0	0.2	0.0	Ce	N/D		N/D		0.1	0.0	0.3	0.2	N/D	
Sc	0.4	0.3	0.2	0.1	0.3	0.4	0.1	0.1	0.2	0.2	Sc	N/D		0.1	0.0	N/D		0.2	0.0	N/D	
Ag	N/D		N/D		0.3	0.0	0.2	0.0	N/D		Y	N/D		N/D		N/D		N/D		N/D	
Sum	109,192.6		123,884.6	-	122,631.4	–	181,600.1	–	93,728.9	–	Sum	20,997.6	–	17,474.0	–	21,665.7	–	62,480.9	–	15,673.2	–

R-W: Residential West; I-N: Industrial North; B-C: Business Center; R-S: Residential South; R-E: Residential East
Elements are order according to the concentration.
SD: Standard deviation.
N/D: Not detectable.
* $p < 0.05$. Differences by site, the Kruskal–Wallis test.
$n = 4$ per site and size.

TABLE 2. Descriptive Statistics for PAHs in PM_{10} and $PM_{2.5}$ Samples

	PM_{10} (ng/mg)											$PM_{2.5}$ (ng/mg)									
	R-W		I-N		B-C		R-S		R-E			R-W		I-N		B-C		R-S		R-E	
PAH	Average	SD	Average	SD	Average	SD	Average	SD	Average	SD	PAH	Average	SD	Average	SD	Average	SD	Average	SD	Average	SD
Acenaphthylene	22.6	7.8	30.8	9.1	22.1	6.9	20.0	4.1	17.8	10.5	Acenaphthylene	13.4	3.8	24.9	15.1	32.7	2.9	17.7	4.2	16.2	4.1
Phenanthrene	10.4	2.3	13.6	3.3	9.6	0.5	14.6	3.3	12.0	4.2	Benzo(b)fluoranthene*	2.8	2.5	13.3	12.4	6.7	6.0	1.2	0.4	0.9	0.6
Benzo(b)fluoranthene*	2.7	0.4	4.9	0.7	3.0	0.7	5.1	1.3	2.4	0.9	Phenanthrene	0.6	1.2	6.0	4.5	4.7	1.6	2.5	0.1	3.4	3.4
Chrysene	1.8	0.4	4.2	0.9	2.0	0.7	3.8	1.1	1.5	1.0	Benzo(g,h,i)perylene	1.5	0.4	2.0	1.9	1.1	0.3	0.9	0.4	1.4	0.4
Benzo(g,h,i)perylene	2.8	2.6	3.0	1.9	1.1	0.6	3.2	1.8	1.7	1.5	Pyrene	0.8	0.2	2.1	0.9	0.8	0.4	0.6	0.3	0.3	0.3
Pyrene*	1.9	0.4	3.6	0.9	1.8	0.7	2.3	1.6	1.3	0.8	Fluoranthene*	0.9	0.2	1.8	0.6	0.8	0.3	0.6	0.2	0.5	0.4
Fluoranthene*	1.3	0.3	2.2	0.6	1.3	0.5	2.3	0.7	0.8	0.5	Chrysene*	0.9	0.6	1.7	0.7	0.7	0.1	0.7	0.2	0.4	0.3
Benzo(k)fluoranthene	1.0	0.4	1.7	0.4	0.8	0.4	1.7	0.6	0.6	0.4	Benzo(k)fluoranthene*	0.4	0.3	0.6	0.4	0.2	0.0	0.3	0.1	0.2	0.1
Dibenzo(a,h)anthracene*	0.9	0.1	0.5	0.6	1.0	0.1	1.1	0.1	0.0	0.0	Dibenzo(a,h)anthracene*	0.0	0.0	0.2	0.5	0.8	0.1	0.3	0.4	0.0	0.0
Benzo(a)anthracene	0.4	0.1	1.2	0.2	0.5	0.2	0.9	0.5	0.4	0.2	Benzo(a)anthracene	0.2	0.1	0.4	0.3	0.1	0.1	0.2	0.1	0.1	0.1
Benzo(a)pyrene	0.2	0.1	0.3	0.2	0.2	0.1	0.2	0.2	0.2	0.0	Benzo(a)pyrene	0.1	0.0	0.1	0.0	0.1	0.0	0.1	0.0	0.1	0.0
Naphthalene	0.0	0.0	0.0	0.0	0.0	0.0	0.0	0.0	0.0	0.0	Anthracene	0.1	0.2	0.0	0.0	0.0	0.0	0.0	0.0	0.0	0.0
Acenaphthene	0.0	0.0	0.0	0.0	0.0	0.0	0.0	0.0	0.0	0.0	Naphthalene	0.0	0.0	0.0	0.0	0.0	0.0	0.0	0.0	0.0	0.0
Fluorene	0.0	0.0	0.0	0.0	0.0	0.0	0.0	0.0	0.0	0.0	Acenaphthene	0.0	0.0	0.0	0.0	0.0	0.0	0.0	0.0	0.0	0.0
Anthracene	0.0	0.0	0.0	0.0	0.0	0.0	0.0	0.0	0.0	0.0	Fluorene	0.0	0.0	0.0	0.0	0.0	0.0	0.0	0.0	0.0	0.0
Indene	0.0	0.0	0.0	0.0	0.0	0.0	0.0	0.0	0.0	0.0	Indene	0.0	0.0	0.0	0.0	0.0	0.0	0.0	0.0	0.0	0.0
Sum	46.0	–	65.9	–	43.3	–	55.2	–	38.5	–	Sum	21.5	–	53.1	–	48.9	–	24.9	–	23.5	–

R-W: Residential West; I-N: Industrial North; B-C: Business Center; R-S: Residential South; R-E: Residential East.
PAHs are order according to concentration.
SD: Standard deviation.
* $p < 0.05$. Differences by site, the Kruskal–Wallis test.
$n = 4$ per site and size.

TABLE 3. Descriptive Statistics for Endotoxin in PM_{10} and $PM_{2.5}$ Samples

	R-W		*I-N*		*B-C*		*R-S*		*R-E*	
Endotoxin (EU/mg)	*Average*	*SD*	*Average*	*SD*	*Average*	*SD*	*Average*	*SD*	*Average*	*SD*
PM_{10}	94.00	67.54	49.68	26.50	82.78	79.69	29.00	10.49	76.98	51.40
$PM_{2.5}$*	6.93	6.48	1.76	1.64	4.05	1.67	30.51	10.13	4.34	2.00

R-W: Residential West; I-N: Industrial North; B-C: Business Center; R-S: Residential South; R-E: Residential East
EU: Endotoxin units.
SD: Standard deviation.
* $p < 0.05$. Differences by site, the Kruskal–Wallis test.
$n = 4$ per site and size.

TABLE 4. Coefficient Loadings of Variables in Each of the Three Principal Components Extracted by Principal Component Analysis

Component 1		*Component 2*		*Component 3*	
Si	0.694	Pyrene	0.937	Zn	0.811
Sr	0.950	Fluoranthene	0.869	S	0.799
Mg	0.921	Li	0.818	Sb	0.792
Ca	0.908	Cr	0.783	Ni	0.759
Al	0.893	Chrysene	0.780	Cu	0.721
Fe	0.787	Benzo(a)anthracene	0.742	Pb	0.665
Endotoxin	0.784	Benzo(b)fluoranthene	0.736	K	0.617
Mn	0.671	Benzo(k)fluoranthene	0.719		
Ba	0.805	As	0.623		

Cutoff point = 0.6.

Significant spatial differences were found for some of the components (Figure 1). For PM_{10}, C_2 and C_3 varied significantly by site ($p < 0.05$). The largest C_2 value was observed in I-N, and the lowest in the R-E site. In the case of C_3, R-S had the highest value and R-W the lowest. C_1 and C_2 present in $PM_{2.5}$ exhibited differences across locations ($p < 0.05$): C_1 was notably higher in R-S, and C_2 had a high contribution in the industrial sector (I-N).

Levels of TNFα and IL-6 Induced by PM_{10} and $PM_{2.5}$

In general, cytokines produced after stimulation of J774A.1 and THP-1 cells with 80 μg/mL of PM_{10} and $PM_{2.5}$, showed a significantly higher response to PM_{10} than $PM_{2.5}$ ($p < 0.05$) (Figures 2 and 3). Most sites had significant differences by size, and some significant differences were observed across sites. $PM_{2.5}$ from the R-S site was the only $PM_{2.5}$ that induced larger TNFα secretion than PM_{10} in J774A.1 cells ($p < 0.05$). IL-6 responses were smaller and more homogeneous than those for TNFα. Although secretion levels in THP-1 cells were lower than in the J774A.1 cells, a similar response pattern was observed with both cell lines ($r = 0.66$, $p < 0.01$ for TNFα and $r = 0.40$, $p < 0.01$ for IL-6).

Cell exposure to 10 μg/mL LPS resulted in secreted levels of TNFα equal to 13,953 ± 2,648 pg/mL by J774A.1 cells and 891 ± 85 pg/mL by THP-1 cells. In the case of IL-6, J774A.1 cells produced 2,100 ± 328 pg/mL whereas THP-1 cells produced 529 ± 53 pg/mL.

Results from the correlation analyses between cytokine production and principal components show that TNFα and IL-6 only had positive correlations with C_1 in both cell lines. The Spearman correlation (ρ) values for TNFα were $\rho = 0.53$ in J774A.1 ($p < 0.01$), and

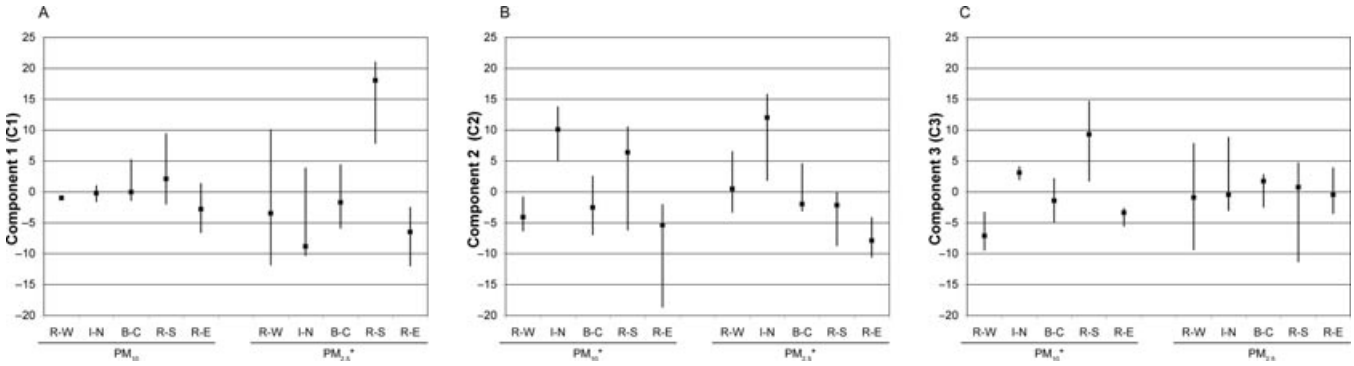

FIGURE 1. Distribution of factor scores in the three principal components found in each site, C_1 (A), C_2 (B), and C_3 (C). The graph displays median, maximum, and minimum values for each component according to site and size. For PM_{10}, statistically significant differences were found among sites for C_2 and C_3. For $PM_{2.5}$, differences were found for C_1 and C_2 ($p < 0.05$, $n = 4$ per size and site, the Kruskal–Wallis test). Statistically significant differences between sites were more frequently observed for I-N and R-S. R-W = Residential West; I-N = Industrial North; B-C = Business-Center; R-S = Residential South; R-E = Residential East. $n = 4$ per site and fraction.

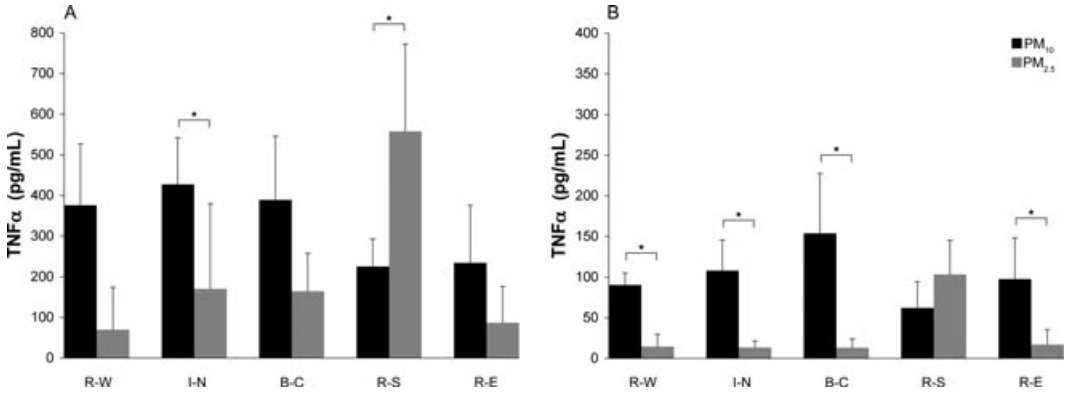

FIGURE 2. Mean (± standard deviation) TNFα levels produced by J774A.1 (A) and THP-1 (B) cells exposed to 80 μg/mL of PM_{10} or $PM_{2.5}$ from five areas of Mexico City: Residential West, R-W; Industrial North, I-N; Business-Center, B-C; Residential South, R-S; Residential East, R-E. Mean of four three-week pool samples obtained by site ± standard deviation. PM_{10} and $PM_{2.5}$ induced statistically significant differences by site in both cell lines ($p < 0.05$, Kruskal–Wallis test). Statistically significant differences by size are indicated in the figure by * ($p < 0.05$, rank test). Significant differences between pairs of sites were more frequently observed with samples from I-N and RS (not marked in the figure).

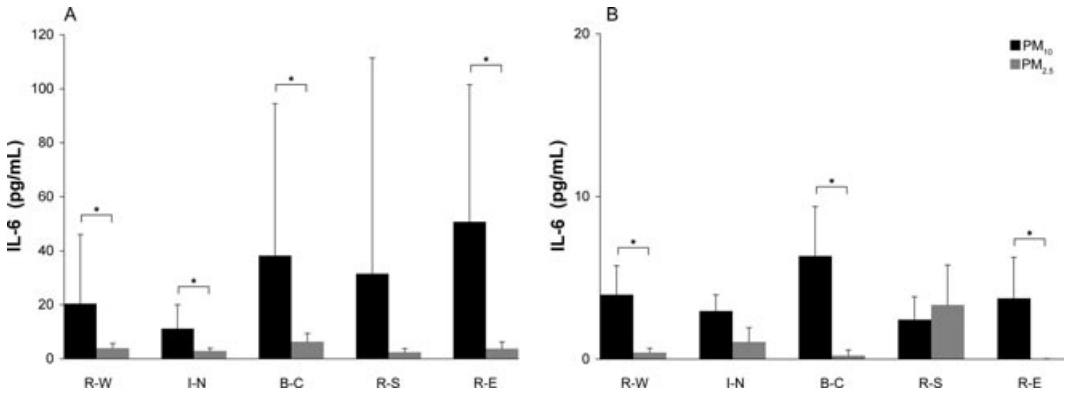

FIGURE 3. Mean (± standard deviation) IL-6 levels produced by J774A.1 (A) and THP-1 (B) cells exposed to 80 μg/mL of PM_{10} or $PM_{2.5}$ from five areas of Mexico City: Residential West, R-W; Industrial North, I-N; Business-Center, B-C; Residential South, R-S; Residential East, R-E. PM_{10} and $PM_{2.5}$ induced statistically significant differences by site in both cell lines ($p < 0.05$, Kruskal–Wallis test). Statistically significant differences by size are indicated in the figure by * ($p < 0.05$, rank test). Significant differences between pairs of sites were more frequently observed with samples from I-N and RS (not marked in the figure).

$\rho = 0.58$ in THP-1 ($p < 0.01$); whereas for IL6, $\rho = 0.31$ in J774A.1 ($p = 0.05$), and $\rho = 0.48$ in THP-1 ($p < 0.01$) (Figure 4). C_2 and C_3 had no correlations with cytokine production.

DISCUSSION

We used PM samples from five Mexico City sites with different predominant air pollution sources to study regional variability in composition and toxicity. Some regions of the city were similar in PM composition and proinflammatory effects, and other regions exhibited clear differences. Regional differences were better understood after conducting PCA and identifying that the proinflammatory effects were strongly related to C_1.

The main compositional differences in PM were between the residential area (R-S) and the industrial area (I-N). PM from R-S had the largest mass explained by the elements studied, whereas PM from I-N was the richest in PAHs.

Exposure of J774A.1 and THP-1 cells to PM_{10} and $PM_{2.5}$ caused secretion of inflammatory cytokines, varying by sampling site and PM size. PM_{10} produced more marked responses than $PM_{2.5}$. In general, TNFα secretion was higher than IL-6 production. Secretion levels from the exposed J774A.1 cells were consistent with previous results from our laboratory [14,15]. Furthermore, we demonstrated that J774A.1 and THP-1 cells react similarly to PM exposure.

We had sufficient samples to conduct an exploratory PCA, which identified three major component classes for PM constituents. The distribution of the three components varied according to location and

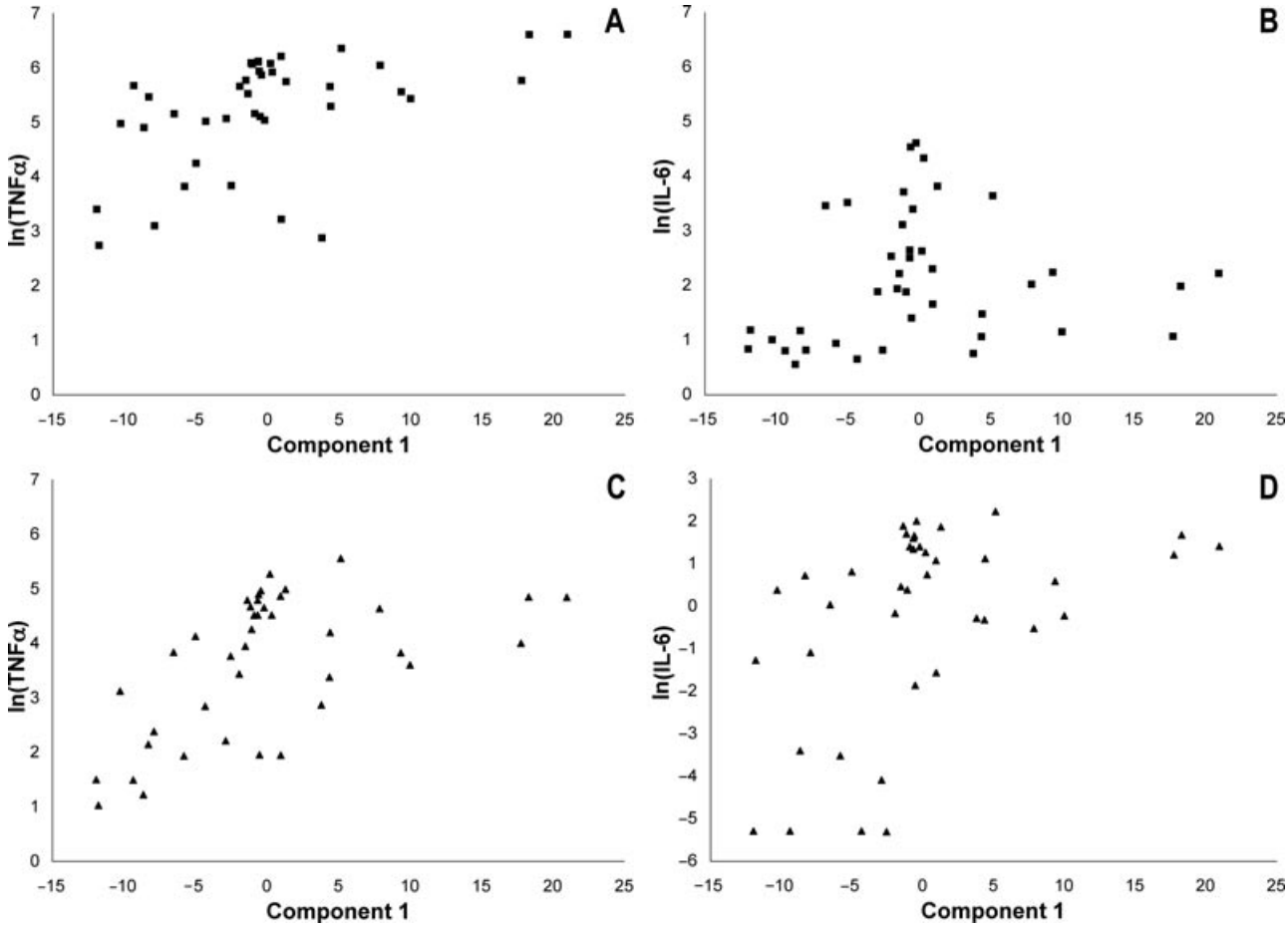

FIGURE 4. Scatter plots showing the correlations found between C_1 and TNFα (A) and IL-6 (B) levels produced by J774A.1 cells. Panels (C) and (D) show TNFα and IL-6 produced by THP-1 cells, respectively [(A) $\rho = 0.53$, $p < 0.01$; (B) $\rho = 0.31$, $p = 0.05$; (C) $\rho = 0.58$ $p < 0.01$, and (D) $\rho = 0.48$ $p < 0.01$. Spearman correlations, $n = 40$].

PM size. C_1 was importantly present in all PM_{10} samples, and mainly present in $PM_{2.5}$ samples from R-S. C_2 was defined by the presence of various PAHs, showing higher levels in both PM fractions from I-N. The C_3 content was higher in PM_{10} from I-N and R-S and homogeneous in $PM_{2.5}$ across the city. As indicated by the positive Spearman correlations, higher concentrations of C_1 were related to increased production of TNFα and IL-6. For instance, the R-S had the largest average values for C_1 and also induced the highest TNFα levels in both cell lines and the highest IL-6 levels in THP-1 cells. This component included elements and endotoxins linked to soil [26–28]. Previous studies from our group support that PM-induced proinflammatory responses result from complex interactions among PM constituents, where endotoxin adds to but does not explain all observed effects [14,29]. These results showing that PM composition associates with cytokine production are consistent with previous reports focusing on the role of PM sources, identifying effects related to groups of chemicals, rather than implicating an individual PM constituent as responsible for observed cellular responses [11–15,28].

Regarding site-related variability in PM composition, spatial differences in PM composition across the city have been also described previously, including a recent rapid change in the southern part of the city, suggesting homogenization of traffic-related sources [23,24,30].

The PAH content of PM was not related to inflammatory potential. Toxicological effects related to PAH (e.g., direct DNA damage) [31,32] need to be evaluated in future studies. The relative participation of each one of the three components identified here by PCA requires further study including a larger set of cell outcomes.

We plan to evaluate whether compositional and inflammatory differences presented here are similar to inflammatory responses among pregnant women living in different zones of Mexico City.

In conclusion, the spatial differences found indicate that the presence of constituents of PM related to

soil sources determine its differential proinflammatory effects.

ACKNOWLEDGMENTS

ICP-MS and HPLC analysis were performed in the Instituto Mexicano del Petróleo (IMP) under the agreement IMP-4278 with the collaboration of Dra. Marina Morán Pineda and Sergio Escalona. We thank the following organizations for making air sampling possible: Gobierno de la Ciudad de México, Red Automática de Monitoreo Atmosférico (RAMA), and Comisión Ambiental Metropolitana. We thank Felipe Ángeles, Beatriz Cárdenas, José García, Martha Hernández, Leticia Martínez, Armando Retama, Nalleli Reyes, Olivia Rivera, Eva Salinas, Laura Sevilla, Jesús Valencia, and Fernando Vega for providing invaluable support.

REFERENCES

1. Pope CA III, Dockery DW. Health effects of fine particulate air pollution: lines that connect. J Air Waste Manag Assoc 2006;56:709–742.
2. Pope CA 3rd, Ezzati M, Dockery DW. Fine-particulate air pollution and life expectancy in the United States. N Engl J Med 2009;360:376–386.
3. Dominici F, Peng RD, Bell ML, Pham L, McDermott A, Zeger SL, Samet JM. Fine particulate matter and hospital admission for cardiovascular and respiratory diseases. JAMA 2006;295:1127–1134.
4. Ghio AJ. Biological effects of Utah valley ambient air particles in humans: a review. J Aerosol Med 2004;17:157–164.
5. Lippmann M. Semi-continuous speciation analysis for ambient air particulate matter: an urgent need for health effects studies. J Expo Sci Environ Epidemiol 2009;19:235–247.
6. Peng RD, Dominici F, Pastor-Barriuso R, Zeger SL, Samet SM. Seasonal analysis of air pollution and mortality in 100 US cities. Am J Epidemiol 2005;16:585–594.
7. Bell ML, Dominici F, Ebisu K, Zeger SL, Samet JM. Spatial and temporal variation in $PM_{2.5}$ chemical composition in the United States for health effects studies. Environ Health Perspect 2007;115:989–995.
8. Dominici F, Peng RD, Ebisu K, Zeger SL, Samet JM, Bell ML. Does the effect of PM10 on mortality depend on PM nickel and vanadium content? A reanalysis of the NMMAPS data. Environ Health Perspect 2007;115:1701–1703.
9. Atkinson RW, Fuller GW, Anderson HR, Harrison RM, Armstrong B. Urban ambient particle metrics and health: a time-series analysis. Epidemiology 2010; 21:501–511.
10. Zanobetti A, Franklin M, Koutrakis P, Schwartz J. Fine particulate matter air pollution and its components in association with cause-specific emergency admissions. Environ Health 2009;8:58.
11. Gilmour MI, McGee J, Duvall RM, Daniels M, Boykin E, Cho SH, Doerfler D, Gordon T, Devlin RB. Comparative toxicity of size-fractioned airborne particulate matter obtained from different cities in the United States. Inhal Toxicol 2007;19(Suppl 1):7–16.
12. Guastadisegni C, Kelly FJ, Cassee FR, Gerlofs-Nijland ME, Janssen NAH, Pozzi R, Brunekreef B, Sandström T, Mudway I. Determinants of the proinflammatory action of ambient particulate matter in immortalized murine macrophages. Environ Health Perspect 2010;118:1728–1734.
13. Steenhof M, Gosens I, Strak M, Godri KJ, Hoek G, Cassee FR, Mudway IS, Kelly FJ, Harrison RM, Lebret E, Brunekreef B, Janssen NAH, Pieters RHH. In vitro toxicity of particulate matter (PM) collected at different sites in the Netherlands is associated with PM composition, size fraction and oxidative potential – the RAPTES project. Part Fibre Toxicol 2011;8:26.
14. Osornio-Vargas AR, Bonner JC, Alfaro-Moreno E, Martínez L, García-Cuellar C, Ponce de León-Rosales S, Miranda J, Rosas I. Proinflammatory and cytotoxic effects of Mexico City air pollution particulate matter in vitro are dependent on particle size and composition. Environ Health Perspect 2003;111:101289–101293.
15. Rosas I, Serrano J, Alfaro-Moreno E, Baumgardner D, Garcia-Cuellar C, Miranda J, Raga G, Castillejos M, Drucker R, Osornio-Vargas A. Relations between PM10 composition and cell toxicity: a multivariate and graphical approach. Chemosphere 2007;67:1218–1228.
16. Kannan S, Misra DP, Dvonch JT, Krishnakumar A. Exposures to airborne particulate matter and adverse perinatal outcomes: a biologically plausible mechanistic framework for exploring potential effect modification by nutrition. Environ Health Perspect 2006;114:1636–1642.
17. O'Neill MS, Osornio-Vargas A, Buxton MA, Sanchez BN, Rojas-Bracho L, Castillo-Castrejon M, Mordhukovich I, Brown DG, Vadillo-Ortega F. Air pollution, inflammation and preterm birth in Mexico City: study design and methods. Sci Total Environ. 2012 Nov 20. pii: S0048-9697(12)01370-8. doi: 10.1016/j.scitotenv.2012.10.079. [Epub ahead of print]
18. Brown DM, Donaldson K, Stone V. Effects of PM10 in human peripheral blood monocytes and J774 macrophages. RespirRes 2004;5:29.
19. Danielsen PH, Moller P, Jensen KA, Sharma AK, Wallin H, Bossi R, Autrup H, Molhave L, Ravanat JL, Briedé JJ, de Kok TM, Loft S. Oxidative stress, DNA damage, and inflammation induced by ambient air and wood smoke particulate matter in human A549 and THP-1 cell lines. Chem Res Toxicol 2011;24:168–184.
20. Alfaro-Moreno E, Torres V, Miranda J, Martinez L, Garcia-Cuellar C, Nawrot TS, Vanaudenaerde B, Hoet P, Ramirez-Lopez P, Rosas I, Nemery B, Osornio-Vargas AR. Induction of IL-6 and inhibition of IL-8 secretion in the human airway cell line Calu-3 by urban particulate matter collected with a modified method of PM sampling. Environ Res 2009;109:528–535.
21. SIMAT (Sistema de Monitoreo Atmosférico). Available at http://www.calidadaire.df.gob.mx/calidadaire/index.php. Accessed December 28, 2012.
22. INE-SEMARNAT (Instituto Nacional de Ecología-Secretaría de Medio Ambiente y Recursos Naturales). Zona Metropolitana del Valle de Mexico. In: Cuarto almanaque de datos y tendencias de la calidad del aire en 20 ciudades mexicanas (2000–2009). México: Instituto Nacional de Ecología; 2011. pp 93–103.
23. Vega E, Ruiz H, Escalona S, Cervantes A, Lopez-Veneroni D, Gonzalez-Avalos E, Sanchez-Reyna G. Chemical

composition of fine particles in Mexico City during 2003–2004. Atmos Pollut Res 2011; 2:477–483.
24. Vega E, Reyes E, Ruiz H, García J, Sánchez G, Martínez G, González U, Chow JC, Watson JG. Analysis of $PM_{2.5}$ and PM_{10} in Mexico City atmosphere during 2000–2002. J Air Waste Manag Assoc 2004;54:786–798.
25. Hair JF, Anderson RE, Tatham RL, Black WC. Multivariate data analysis with readings. New York: MacMillan; 1992.
26. Moffet RC, Desyaterik Y, Hopkins RJ, Tivanski AV, Gilles MK, Wang Y, Shutthanandan V, Molina TT, Abrahamn RG, Johnson KS, Mugica V, Molina MJ, Laskin A, Prather KA. Characterization of aerosols containing Zn, Pb, and Cl from an industrial region of Mexico city. Environ Sci Technol 2008;42:7091–7097.
27. Querol X, Pey J, Minguillon MC, Perez N, Alastuey A, Viana M, Moreno T, Bernabe RM, Blanco S, Cardenas B, Vega E, Sosa G, Escalona S, Ruiz H, Artiñano B. PM speciation and sources in Mexico during the MILAGRO-2006 campaign. Atmos Chem Phys 2008;8:111–128.
28. Veranth JM, Moss TA, Chow JC, Labban R, Nichols WK, Walton JC, Watson JG, Yost GS. Correlation of in vitro cytokine responses with the chemical composition of soil-derived particulate matter. Environ Health Perspect 2006;114:341–349.
29. Osornio-Vargas AR, Serrano J, Rojas-Bracho L, Miranda L, Garcia-Cuellar C, Reyna MA, Flores G, Zuk M, Quintero M, Vazquez I, Sanchez-Perez Y, Lopez T, Rosas I. In vitro biological effects of airborne $PM_{2.5}$ and PM_{10} from a semi-desert city on the Mexico-US border. Chemosphere 2011;83:618–626.
30. Chow JC, Watson JG, Edgerton SA, Vega E. Chemical composition of PM2.5 and PM10 in Mexico City during winter 1997. Sci Total Environ 2002;287:177–201.
31. Garcia-Suastegui WA, Huerta-Chagoya A, Carrasco-Colin KL, Pratt MM, John K, Petrosyan P, Rubio J, Poirier MC, Gonsebatt ME. Seasonal variations in the levels of PAH-DNA adducts in young adults living in Mexico City. Mutagenesis 2011;26:385–391.
32. Oh SM, Kim HR, Park YJ, Lee SY, Chung KH. Organic extracts of urban air pollution particulate matter ($PM_{2.5}$)-induced genotoxicity and oxidative stress in human lung bronchial epithelial cells (BEAS-2B cells). Mutat Res 2011;723:142–151.